University of Tennessee, Knoxville

Trace: Tennessee Research and Creative Exchange

Chancellor's Honors Program Projects

Supervised Undergraduate Student Research and Creative Work

5-2020

Techno-economic Analysis on the Recovery & Valorization of Lithium from Recycled Battery Waste Materials by Hydrometallurgical Methods.

Preston N. Nicely
pnicely1@vols.utk.edu

Noah Dunlap
University of Tennessee, Knoxville

Joseph Swann
University of Tennessee, Knoxville

John Hill
University of Tennessee, Knoxville

Follow this and additional works at: https://trace.tennessee.edu/utk_chanhonoproj

Part of the Process Control and Systems Commons

Recommended Citation

May 4, 2020

Dr. Robert Counce
CBE 488: Honors Design Internship in Green Engineering
University of Tennessee, Knoxville

Dear Dr. Counce:

We are submitting the following report entitled *Techno-economic Analysis on the Recovery & Valorization of Lithium from Recycled Battery Waste Materials by Hydrometallurgical Methods.*

The attached report details the capital and manufacturing costs for designing a separation process of spent lithium ion battery components.
I hope you find the report satisfactory.

Sincerely,

John Hill

Preston Nicely

Noah Dunlap

Joseph Swann

Honors Design in Green Engineering
University of Tennessee
Knoxville, Tennessee

Enclosure:
Final Report

Techno-economic Analysis on the Recovery & Valorization of Lithium from Recycled Battery Waste Materials by Hydrometallurgical Methods

CBE 488: Honors Design Internship in Green Engineering

Group 6

John Hill
Joseph Swann
Noah Dunlap
Preston Nicely

Chemical and Biomolecular Engineering Department
University of Tennessee Knoxville
1331 Circle Park Drive SW, Knoxville, TN, 37916

1

Table of Contents

1.0 Introduction

Lithium Ion Batteries (LIBs) have been used since the 1990's to power portable electronic equipment. Furthermore, the recent adoption of Electric Vehicles (EV's) and Plug-In-Hybrids (PIH's) has increased the demand for LIBs. This is largely due to the higher specific energy and specific power range achievable by LIBs as compared to either nickel metal hydride or lead-acid batteries as shown in Figure 1.
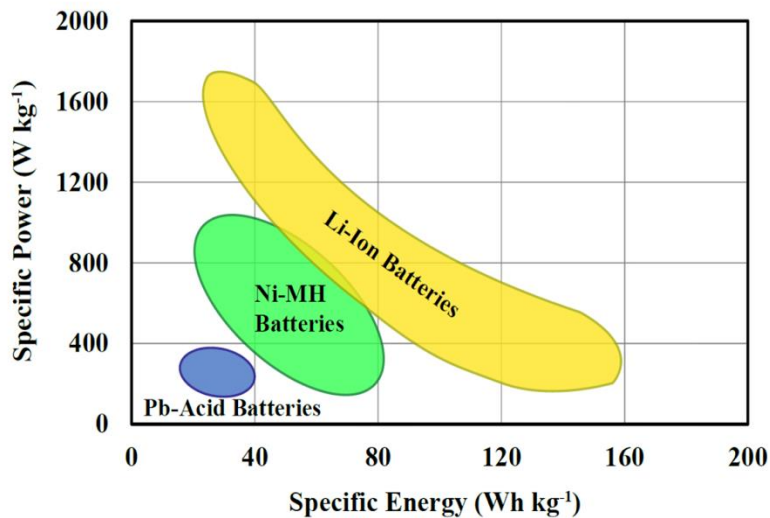
Figure 1: Ragone Plot of Power & Energy Ranges for LIBs (Heidari, K.H., et. al)

LIBs use $LiXMa_2$ electrodes with some examples being $LiMn_2O_4$, $LiNiO_2$, and most commonly $LiCoO_2$. Nearly 28 wt% of a typical LIB is $LiCoO_2$ [1]. Though lithium can be obtained in several different forms, lithium carbonate (Li2CO3) is more commonly used as a feedstock in the production of lithium ion batteries [6]. Choubey et al. predict that by the year 2025, global demand for lithium carbonate will increase to nearly half a million tons per annum, causing a shortage by 2023. Considering that batteries maintain a significantly higher lithium composition than that of natural deposits, many researchers have urgently pushed the formation of a circular lithium economy to mitigate price insecurity that could be caused by limited supplies [14].

Currently, the high market price of cobalt and manganese has persuaded the industry to introduce batteries as a feedstock into the existing large-scale (usually pyrometallurgical) recovery processes. Cobalt and manganese yield roughly 35,000 and 20,000 $/tonne on the commodities market, respectively [15]. Lithium can be recovered from these processes, but because of its currently low market price, it is often left in the slag [3].

The design objectives for this project are fourfold: to summarize and provide recommendations for LIB separation and recovery schemes, to develop an original process flow diagram, to conduct a capital and manufacturing cost analysis, and to optimize the purity and recovery of valuable elemental battery components. The scale of this process will include a raw material stream in the form of spent lithium batteries at a flow rate of 1,000 kg/hr. The cost analysis will be based on a class 4 economic estimate and should fall within an error range of +30% to -20% of the actual cost to implement and run the separation process. The economics investigated within this report will be based on a reference ChE index of 599.5 (2019). Based on the design put forward by Castillo, products should be nearly 100% pure and in their metallic hydroxide form. Major and minor hazards should be accounted for in the design of each step, and the overall environmental impact should fall within EPA standards with a goal of reducing the carbon footprint of the plant.

This project is sponsored by JSW Fund for Undergraduate and Graduate Research at the University of Tennessee (UT). Our contacts are Drs. J. S. Watson and R.M. Counce at the University of Tennessee, Knoxville. Important review articles are by Xu et al (2008), Zeng et al. (2014), Heidari et al. (2018), and Liu et al. (2019).

2.0 Synthesis Information for Processes

2.1 Valorization Process Schematic

In our design process of lithium recovery, battery components (e.g. lithium, manganese, iron) are washed, crushed thoroughly, and then allowed to dissolve in a tank of water, producing hydrogen gas, metal hydroxides, and lithium ions in solution. From there, the aqueous solution is sent to a filter where nearly all the non-lithium species are extracted. The remaining lithium solution is sent to an evaporator to retrieve lithium hydroxide. The precipitant consisting largely of Iron, Cobalt, Nickel, Chromium, and Manganese is sent to an acid dissolving step at pH 4.3 for roughly 2 hours. Nitrogen and oxygen gas are evolved and exhausted to the atmosphere. Ferric hydroxide is precipitated and filtered off for processing into steel. The pH is increased incrementally as nickel, cobalt, and manganese precipitates are filtered off. Upon final evaporation, sodium chromate is precipitated and recovered. Finally, the remaining aqueous solution is sent to waste treatment while our desired lithium product as well as the byproducts can all be further processed and sold as pure metallic species.
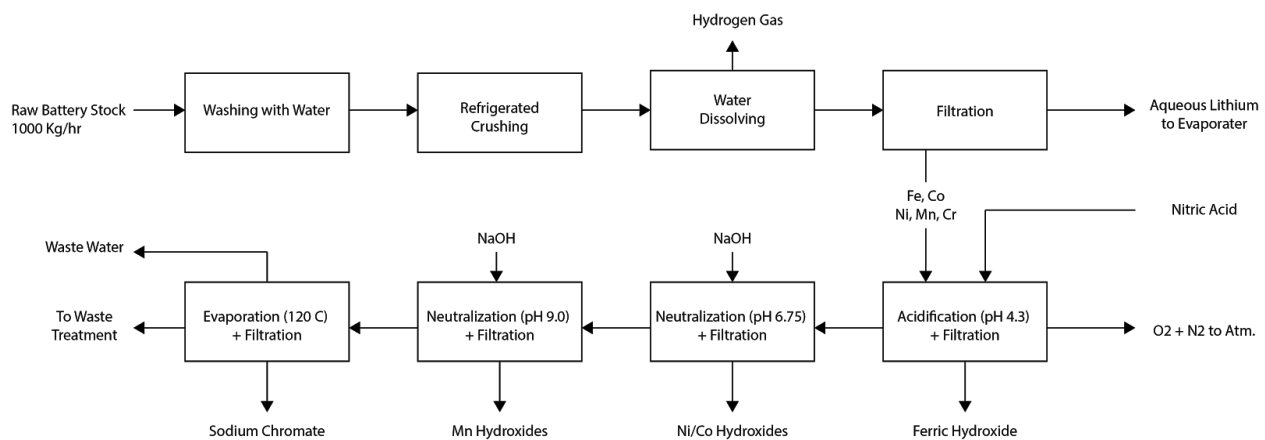
Figure 2: Block Diagram for the Recovery of Elemental Lithium

2.2 Identify constraints

Throughout this report, there are a plethora of constraints on the LIB recycling process that must be considered and handled appropriately when making technological and economical recommendations for the optimization of this process for future industrial applications. It was found that the major constraint was elemental composition of the battery. Despite the common usage of $LiCoO_2$ batteries, $LiMn_2O_4$ batteries were used as the main precursor compound for this separation process in accordance to Castillo et al.'s experimental discoveries. The specific elemental composition of this type of battery is recorded in Table 1.

Table 1: Quantitative Analysis of Metallic Part of Lithium Cells (Castillo, et. al)

Elements	Cylindrical cell concentration (wt% $\pm$ 0.2)	Button cell concentration (wt% $\pm$ 0.2)	Average Concentration (wt% $\pm$ 0.2)
Li	1.5	1.8	1.65
Mn	9.6	16.4	13
Co	0.1	0.1	0.1
Fe	34	41.3	37.65
Ni	5.4	3.0	4.2
Cr	9.6	9.6	9.6
Mo	0.8	0.1	0.45

While our process is based on these compositions., additional components, such as aluminum, copper, and molybdenum, can lead to contamination issues. For example, aluminum will tend to dissolve/precipitate in and out of solution along with the lithium [4], so large amounts of aluminum containing batteries can decrease the purity of the final lithium hydroxide product. Similarly, considerations must be made as to the level of isolation and purity of each elemental

component. In other words, we would like to isolate each species separately, rather than collect all of them together. All this places a constraint on the types of batteries and their elemental compositions that are most successful in the separation process detailed in this report.

2.3 Chemical Equations

The vast majority of reactions follow the following ionic-hydroxide association/dissociation scheme where "Me" is the ionic metal:

Equation 1: $Me^{n+}(aq) + nOH^-(aq) \rightleftharpoons Me(OH)_n(s)$
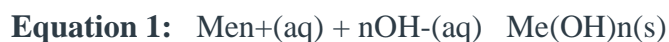
However, according to the OLI simulation, the lithium hydroxide stream does contain aqueous lithium hydroxide, but because of its electromagnetic similarity to water, it does not precipitate until evaporation. Interestingly, upon the final process stream evaporation, sodium chromate precipitates from solution according to the following reaction:

Equation 2: $2Na^+(aq) + CrO_4^{2-}(aq) \rightleftharpoons Na_2CrO_4(s)$

Chromium thermodynamically forms into its aqueous oxide ion, which makes it particularly difficult to remove from any solution. Luckily, it is the final elemental battery component to be removed in our process.

2.4 Brief Literature Summary

A.   *Types of Lithium Ion Batteries (LIBs)*

Over time, various lithium ion batteries have been developed and used for a variety of practical purposes. One of the first types of LIB's is Lithium Cobalt Oxide ($LiCoO_2$ or LCO), which has a very high specific energy making it useful for cameras, laptops, and phones. However, $LiCoO_2$ batteries have a short life span, low thermal stability, and have restrictive loading

capacities. LiMn$_2$O$_4$ batteries (LMO) are the batteries studied in this report and are capable of lower internal resistances and current handlings. This allows LMO batteries to charge fast, making them beneficial for use in power tools, medical equipment, and hybrid and electrical vehicles. Additionally, the spinel structure of LMO batteries accounts for its lowered resistance and allows for a more moderate specific energy compared to LCO batteries [13].

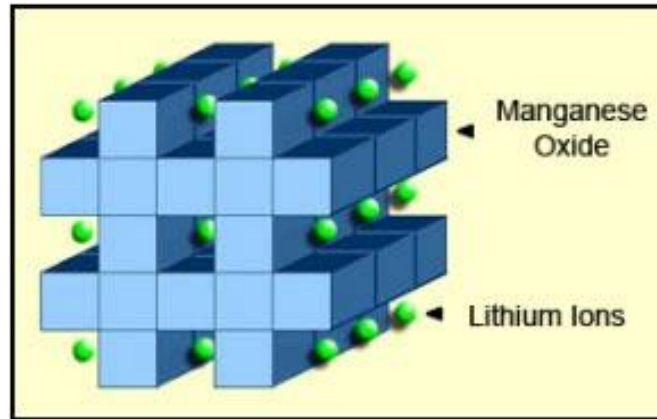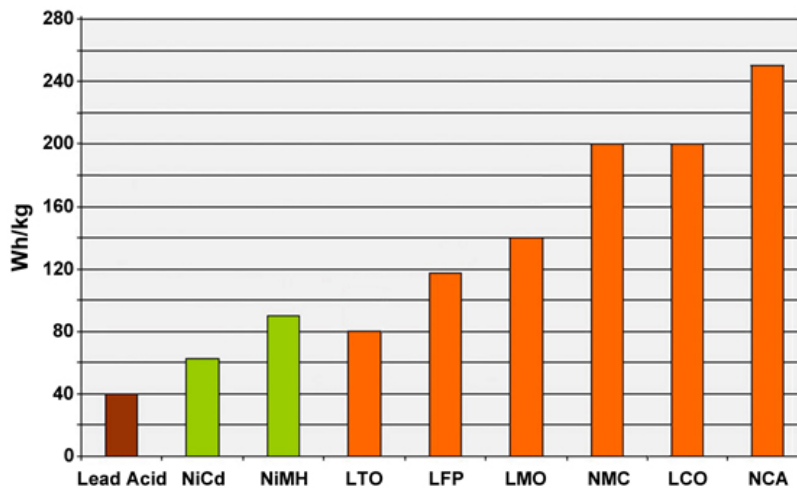*Figure 3: LMO Battery Structure (Battery University)*

Figure 4: Specific Energy Capabilities for Various Lithium Ion Battery Subtypes

In recent years, the advancements of this industry have led to the production of NMC and NCA batteries which have shown to be even more beneficial and efficient than their LCO or LMO counterparts. NMC batteries combine nickel with manganese which allows these batteries to have

high energy (from the nickel) and high stability (from the manganese). The composition of NMC batteries usually results in 5 parts Nickel, 3 parts Cobalt, and 2 parts Manganese. These batteries are typically used in electric power trains and some power tools [13]. Figure 4 highlights the differences in specific energy capacities across a range of LIBs.

B. LIB's Structure & Mechanism of Energy Storage

Within a typical battery system, there are three components: the negative electrode (anode), the positive electrode (cathode), and the aqueous/non-aqueous electrolyte. These components can be structured into various battery container shapes including cylindrical, button, and pouch cells [13]. Electrical energy is generated when common ions like Li+ flow from one electrode to another across the electrolyte medium. This transient movement of ions creates a polarized system in which electrochemical reactions produce electrons which in turn produce electricity. The state of the electrolytes and the electrodes can vary across different batteries. The most important material in a LIB is the cathode material. During the charging and discharging cycles of the battery when the Li+ ions are flowing, the oxidation-reduction reactions that are taking place could have an adverse effect on the compositional status of the cathode material. To prevent this, it is imperative that the LIB have a stable, crystalline structure to it. In the case of this study on $LiMN_2O_4$ (LMO) LIBs, the cathodes in these batteries are spinel oxides, a three dimensional framework that increases the flow of ions through the electrolyte. This unique structure allows for less damage to the battery structure during charging/discharging cycles [4].

C. Lithium Recovery Process

Lithium ion batteries are largely recovered by two different methodologies: hydrometallurgical-dominant processes and pyrometallurgical-dominant processes. As the name

suggests, pyrometallurgical-dominant processes utilize high temperatures to separate cobalt and nickel from mixtures, however lithium and manganese are lost to the process's slag. Hydrometallurgical-dominant processes rely on leaching, precipitation, and filtering to deconstruct the mixtures. Castillo et al. present a hydrometallurgical approach to recover the individual elemental components of lithium ion batteries. As is common, this approach utilizes mechanical separation then acid/base chemistry and filtering.

Xu, et. al also proposes hydrometallurgical methods for the separation of LIBs. In his report, Xu details the physical (mechanical, thermal, mechanochemical, and dissolution treatments) and chemical (acid leaching, bioleaching, solvent extraction, chemical precipitation, and electrochemical processing) recycle processes for the spent LIBs. Xu also notes that Castillo utilizes a combination process for the recycling "based on simple and environmentally compatible operations". [5] These combinations are the crushing, acid leaching, heat treatment, and chemical precipitation. The flowsheet for the combined processes used by Castillo is detailed in Figure 5. Xu then continues to describe different typical combinations of these steps others have performed, however these are not considered in this process.
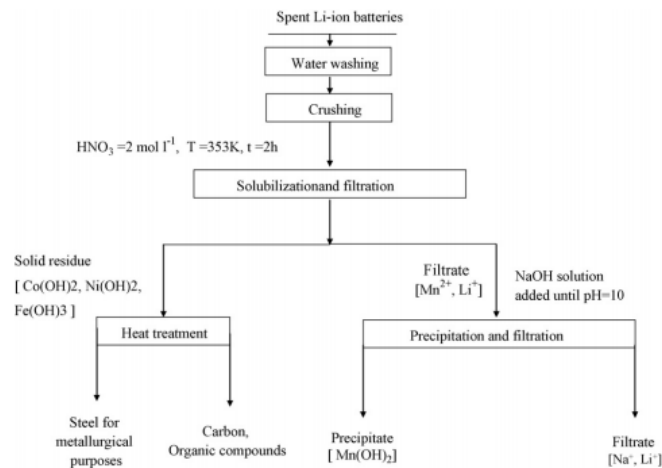

Figure 5: Flow sheet for the combined recycling processes utilized by Castillo as described by Xu

D. Unit Operation Recommendations

The valorization process of recovering spent Lithium from LIBs includes the recovery, repair, and regeneration of viable Lithium [3]. Liu states that prior to pre-treating the spent LIBs, they must be discharged to prevent short circuiting and self-ignition during the crushing of the batteries. The dismantling of the batteries is usually done by crushing or shredding, where unnecessary casing components are filtered out via magnetic or air separation techniques [3]. Zeng argues that the LIBs should be immersed in a salt solution to prevent short-circuiting and then the inner components should be immersed in liquid nitrogen for 4 minutes. He claims these cryogenic methods are imperative for maintaining optimal safety precautions [6]. Lee et al recommends similar protocols for the pre-treatment of LIBs with an alternating thermal treatment and high-speed shredding technique. He proposes that the spent LIBs are treated at 100-500 C for 30 minutes, shredded at high-speeds to a 5-20 mm size powder, thermally treated at 300-500 C for 30 minutes, filtered via a vibrating screen, and then heated in a calcination reaction at 700-900 C for approximately 1 hour. This additional calcination reaction is imperative based on Lee's recommendations to limit the supply of air to the LIBs at this stage (Lee et al). Even with proper precautions, once the batteries are opened they have a certain chance to rapidly heat. This can be combated by refrigeration of the battery during the crushing step specifically. Utilizing cooling techniques is also advisable to combat safety hazards present using this process. However, it is difficult to incorporate refrigeration techniques into some of the equipment like the crusher, therefore, when designing this specific type of equipment, extra caution should be held.

Both Castillo and Liu analyze the effect of using different acids when dissolving the spent batteries. The acid concentration and the dissolution agent will heavily influence the recovery of the metals. The purpose of this step is to maximize this recovery and solubilization of the LIBs in

the acid media. Castillo studied hydrochloric acid (HCl) and nitric acid (HNO₃), with concentrations varying between 0.1 - 5.0 mol L-1. Figures 6 and 7 show how the recovery of Lithium varies with the acidification reaction time. Based on this data, it was determined that dissolving LIBs in nitric acid is more efficient as nearly 100% recovery was achievable in a shorter span of time (~2 hours).
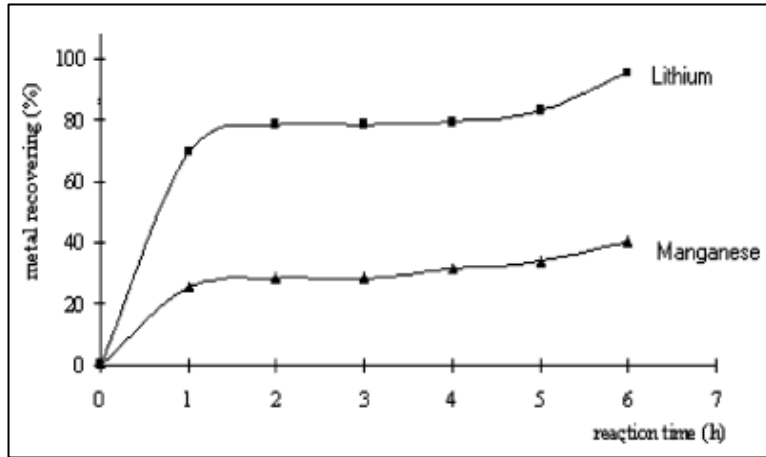
Figure 6: Metals recovery (%) vs dissolution time in hydrochloric acid
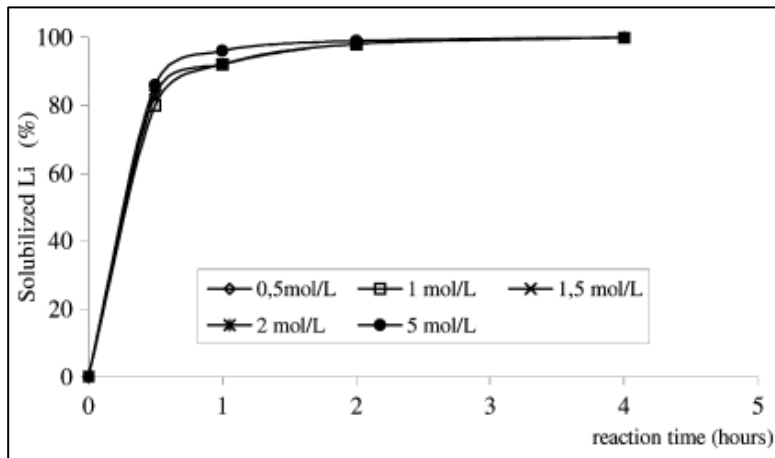
Figure 7: Metals recovery (%) vs dissolution time in nitric acid

Liu is largely in accordance with the findings presented with Castillo. He also mentions the use of other strong organic acids such as citric acid, formic acid, malic acid, aspartic acid, ascorbic acid, oxalic acid, and glycine as other possible chemicals capable of leaching out the desirable cathode

materials. Additionally, Liu acknowledges that the kinetics of the leaching process are dependent on the type of leachent, the reduction concentrations, agitation speeds, temperatures, residence times, and the solid to liquid ratio of the filtration steps.

3.0 Relevant Information & Basic Economics

3.1 Tables of product, byproduct, energy, and raw material costs and specifications

Lee and Rhee deconstruct the average LIB feedstock by elemental composition, however only cobalt including LIB's were considered. Manganese is another major component of LIB"s with a high market price and should be considered when determining the feedstock composition, especially since it is of high consideration in this report.

Table 2: Material Cost Assumptions [15]

Material	Cost/Unit
Spent LIBs	$0/ton
68% Nitric Acid	$300/ton
Sodium Hydroxide	$125/ton
Aluminum (Al)	$2,000/ton
Copper (Cu)	$6,300/ton
Iron (Fe)	$100/ton
Cobalt (Co)	$35,000/ton
Molybdenum (Mo)	$26,000/ton

Lithium Carbonate (Li_2CO_3)	$8,750/ton
Manganese (Mn)	$2,000/ton
Lithium Hydroxide (LiOH)	$15,000/ton
Lithium Oxide (Li_2O)	$50,000/ton

3.2 Thermodynamic Properties Estimation

Essentially all of the reactions taking place in this process are aqueous redox chemistry based. OLI Flowsheet's ability to perform these types of calculations was a major motivation in its application to this project. In OLI FLowsheet, the aqueous (H+ ion) thermodynamic framework was used, including the alloys (Aq), low temperature (Aq), ion exchange (Aq), and aqueous (H+ ion) databanks, though it is not apparent if the alloy's database really is necessary. Naturally, redox chemistry of all ionic species for all phases was included in the simulation. It should be mentioned that each reactor relied on a stoichiometric conversion to simulate reactions rather than experimentally defined kinetics, but with rather simple process reactions this was appropriate.

4.0 Results

4.1 Optimization

Our process outlines a separation hydrometallurgical process, therefore the optimization seeks to maximize the recoveries and separation of individual elemental components, while keeping capital and annualized costs low. Ideally, each elemental species would be separated into its own stream without contaminants and with a recovery of 100%. It is clear from Castillo et. al's work that lithium recovery is the most environmentally important, but for the profitability of

the process, other high value metals need to be refined including cobalt, nickel, chromium, iron and manganese.

Changes to the Suggested Valorization Scheme

Castillo's valorization process did in fact recover nearly all the lithium, however, in practice, since lithium is the last of the metals to be recovered, the outlet stream is contaminated heavily with residual process species such as sodium and nitrates. While it is possible to remove the lithium via reactive precipitation, it was found during development that lithium could be removed cleanly if it was the first species to be removed rather than the last. The reactions resulting from the addition of crushed elemental battery components to clean water evolves hydrogen gas and increased pH. At high pH (usually greater than 10), lithium is the only free metallic ion in solution, so all other species can be filtered off and sent through the traditional valorization process. The lithium-only solution can be sent to the evaporator for the production of lithium hydroxide (as was chosen here), or lithium carbonate can be reactively precipitated by sparging with carbon dioxide.

Reactor 1:

The reaction between the battery species and water should be conducted adiabatically but will produce their own heat. Though the process was simulated in OLI Flowsheet's stoichiometric conversion reactor, it was estimated that a residence time of two hours would be sufficient for dissolving all the lithium since similar times were recommended by Castillo et al. with regard to the dissolving of metals in nitric acid. Molybdenum is not always a component of batteries but is included in our analysis. OLI tells us that Nearly all the molybdenum forms MoO3 in this reactor but remains in solution and will inevitably end up in the lithium rich stream. However, the data

regarding MoO3's thermodynamics were not retrievable by OLI at the time of this simulation, so it is difficult to tell if this is actually an impurity or not.

Reactor 2:

The second uses a dilute nitric acid solution to dissolve the remaining metal species and decrease the pH, adiabatically. Castillo recommended heating the reactor to 80 degrees celsius, but it was found that by using the condensed process water from the lithium only stream (T = 95 C), the reactor would settle around 85-86 degrees celsius without additional heating. The pH was set to roughly 4.2, following Castillo's guidelines, which is low enough to keep all but the ferric species from precipitating. A large amount of water vapor, nitrogen gas, and oxygen gas are produced in this reactor and can be exhausted to the atmosphere. There are no carbon emissions in this exhaust. Ferric acid recovery after filtration is nearly 100% and practically pure.

Neutralizer/ Filters 1 and 2:

The first neutralizer uses sodium hydroxide to raise the pH to 6.75, rather than the 6.5 which Castillo et al. recommended. The slight increase to pH allows for a highest yield of nickel and cobalt hydroxides, without the accidental precipitation of manganese species. After filtration, there should be no detectable Manganese and the recoveries for nickel and cobalt are 99.75% and 97.43%, respectively. Unfortunately, nickel and cobalt species cannot be easily removed individually without the addition of additional neutralizer/filtration equipment. Similarly the second neutralizer increases the pH to 9 as opposed to the suggested 10, which decreases the amount of sodium hydroxide used and improves the safety and longevity of the process. However, a nearly complete precipitation of manganese hydroxide can be achieved at this pH. The product stream is practically pur with a 99.7% recovery.

Sodium Chromate Recovery:

Interestingly, upon the evaporation of process water, sodium chromate formed and precipitated out. In the interest of increasing the economic potential for our process, this product should be collected and sold. Unfortunately, the remaining chromium (about 70%) cannot be recovered as easily and serves as a point of improvement to our proposed process schematic.

Hydrogen Gas Energy Recoup:

Reactor one forms roughly 28.2 kg per hour of hydrogen gas with a 97.7 mol % purity. The balance is water vapor. This hydrogen stream can be burned to produce clean electricity upon the installation of a steam turbine. While the combustion of hydrogen can produce up about 1.1 MW, steam turbines of this capacity can usually only recover half of that energy. Assuming this, the proposed plant can recuperate about 517 kW of electrical energy or roughly $496,000 annually. At roughly 900 $/kW, this generator will pay for itself in roughly one year.

4.2 Process Flow Diagram

The overall process flow diagram is shown below and was generated in OLI flow sheet.
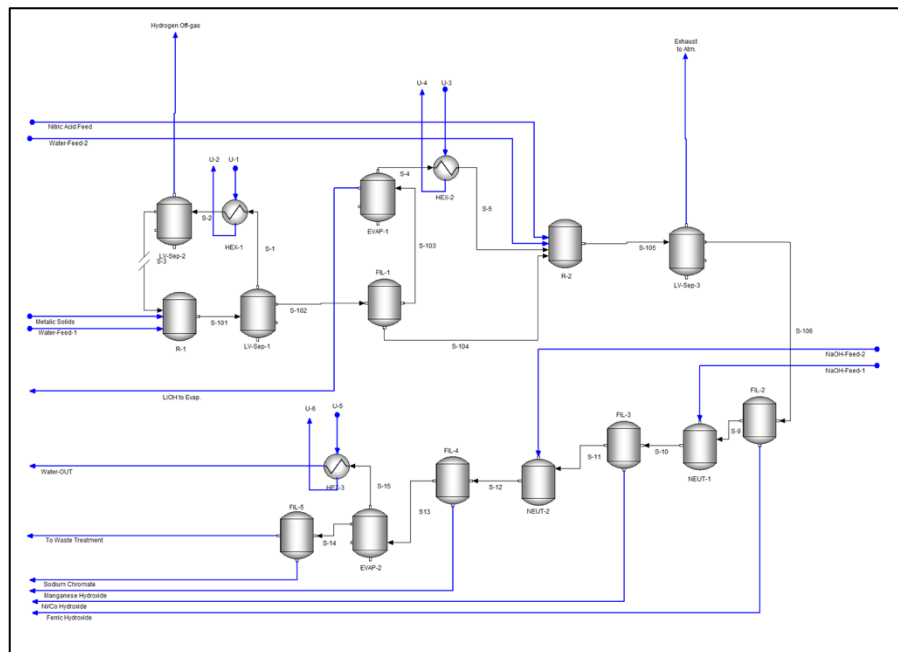
Figure 8: OLI Lithium Recovery Process Flow Diagram

4.3 Safety, Health and Environment Analysis

When designing our extraction of LiOH from LIBs, it was imperative to consider Principles of Inherently Safer Design (ISD). The fundamental principles behind this approach are to substitute, minimize, moderate, and simplify. The principles of ISD should be applied throughout all aspects of the chemical manufacturing industry and design process. For instance, ISD principles need to be applied for chemical selection, process technology development, manufacturing site selection and layout, building the facility, and improving the facility. When applicable, it is best to replace any unnecessary chemicals or materials with less hazardous ones. Also, moderate temperatures, pressures, and quantities of materials should be considered when product quality or yield is not hindered. The hydroxide byproduct streams that are recovered from our process should be sent to separate holding containers to avoid contamination and undesirable mixing. Additionally, the process has been simplified down as much as possible to still produce high quality separation of all the desirable materials. The final waste stream that is produced at the end of our process is to be discharged to a proper waste treatment facility to dispose of the unnecessary compounds. For environmental impacts, the plastic coverings and other battery casing material harvested from the crushing and filtering stages of our process will be collected and recycled to minimize waste.

A short FMEA (failure mode effect analysis) on any of the unit vessels in our process would demonstrate the principles of ISD that were clearly upheld in the design of our flowsheet. For instance, when considering the crusher at the beginning of the flowsheet, it is important to gauge the risk of a fire hazard due to excess heating caused by static discharging of the crushed batteries. Without proper safety features, this potential fire hazard (i.e failure mode) would likely score a 10 for severity, a 4 for occurance, and a 3 for detection, resulting in an overall chance of

risk at around 12%. In order to reduce this chance of failure even further, special considerations like excess cooling of the batteries in water as well as extending the batch lag time to avoid overuse of the crusher could help reduce that risk probability number even further [11].

4.4 Capital cost estimates

Capital costs were estimated using charts in Dr. Gale Ulrich's textbook, *Chemical Engineering Process Design and Economics: A Practical Guide*. Using estimated process vessel and heat exchanger dimensions, base costs were found on Ulrich's graphs and multiplied the cost by material and pressure factors, as well as the current ChE Index of 599.5. The results are tabulated below [12]. The total grassroots capital required for the proposed layout is $7,353,156.

Table 3: Capital Cost Summary

CAPITAL COST SUMMARY   Date to which estimate applies: Mid-2020

Job title: Lithium Recovery from Recycled Li-Batteries   Location: TBD   Capacity: 1,000 kg/hr   By Noah Dunlap

Cost Index Type: CE Plant Cost Index Cost Index Value: 599.5   Date 4/14/2020

Equipment Identification	Number	Capacity or Size Specifications	Purchased Equipment Cost Year 2004	Purchased Equipment Cost Target Year*	Bare Module Factor, F_{BM}	Base Bare Module Cost, C_{BM}	Material Factor, F_M	Pressure or other Factors, F_P	Actual Bare Module Factor, F_{BM}	Bare Module Cost, C_{BM}	Total
Auxilliary Facilities											
	N/A										
Total Auxilliary Facilities											
Crushers, Mills, Grinders											
Crusher	C1	0.277 kg/sec, carbon steel	16000	23980	2.1	50358	1	1	2.1	50358	
Total Crushers, Mills, Grinders						50358					50358
Heat Exchangers											
Heat Exchanger	HEX1	265.64 m2, carbon steel, hairpin multitube 10 barg	25000	37468.8	3.2	119900	1	1	3.2	119900	
Heat Exchanger	HEX2	1004.43 m2, carbon steel, hairpin multitube 10 barg	60000	89925	3.2	287760	1	1	3.2	287760	
Heat Exchanger	HEX3	629.29 m2, carbon steel, hairpin multitube 10 barg	42000	62947.5	3.2	201432	1	1	3.2	201432	
Total Heat Exchangers						609092					609092
(Other items as taken from the equipment list)											
	N/A										
Process Vessels											
Reactor	R1	1 m ID x 12.05 m vertical, carbon steel	25000	37468.8	3.2	119900	1	1	3.2	119900	
Reactor	R2	1.5 m ID x 8.97 m vertical, carbon steel	28000	41965	3.2	134288	1	1	3.2	134288	
Neutralizer	N1	1.5 m ID x 7.47 m vertical, carbon steel	23000	34471.3	3.2	110308	1	1	3.2	110308	
Neutralizer	N2	1.5 m ID x 8.07 m vertical, carbon steel	26000	38967.5	3.2	124696	1	1	3.2	124696	
Evaporator	E1	1 m ID x 10.57 m vertical, carbon steel	23000	34471.3	3.2	110308	1	1	3.2	110308	
Evaporator	E2	4 m ID x 24.55 m vertical, carbon steel	140000	209825	3.2	671440	1	1	3.2	671440	
Tower Total						1270940					1270940
Filters											
Filter	F1	1.43 kg/s, carbon steel	190000	284763	2	569525	1	1	2	569525	
Filter	F2	2.09 kg/s, carbon steel	210000	314738	2	629475	1	1	2	629475	
Filter	F3	1.92 kg/s, carbon steel	200000	299750	2	599500	1	1	2	599500	
Filter	F4	1.96 kg/s, carbon steel	200000	299750	2	599500	1	1	2	599500	
Filter	F5	0.26 kg/s, carbon steel	110000	164863	2	329725	1	1	2	329725	
Total Pumps						2727725					2727725
Storage Vessels											
LV-Separator	S1	8.89 m3, carbon steel, vertical bullet tank, 0-10 barg	12000	17985	2.1	37768.5	1	1	2.1	37768.5	
LV-Separator	S2	0.19 m3, carbon steel, vertical bullet tank, 0-10 barg	3000	4496.25	2.1	9442.125	1	1	2.1	9442.13	
LV-Separator	S3	13.51 m3, carbon steel, vertical bullet tank, 0-10 barg	28000	41965	2.1	88126.5	1	1	2.1	88126.5	
Total Storage Vessels						135337.13					135337.125

Total bare module cost	Base materials, $C_{TBM} = \Sigma\, C_{BM} =$ **$4,793,452**	Actual materials, $C_{TBM} = \Sigma\, C_{BM} =$ **$4,793,452**
Contingency and fee		$C_C + C_F = C_{TBM} \times 0.18 =$ **$862,821**
Total module cost		$C_{TM} =$ **$5,656,274**
Auxiliary (offsite) Facilities		$C_{TBM} \times 0.30 =$ **$1,696,882**
Grass Roots capital		$C_{GR} =$ **$7,353,156**

*2004 cost x (Target Year Cost Index/2004 Cost Index)
**For an example of a completed capital cost summary, see Table 5-7.

19

4.5 Manufacturing Cost Estimates

Manufacturing costs were estimated based on the materials required to run daily operations at a plant recycling LI batteries. It was assumed that batteries could be sourced for free, as they are not useful outside of their standard life span. Additionally, the by-product credit discussed in 4.1 has been applied to the total. The net annual profit was found to be $506, 933.

Table 4: Manufacturing Cost Summary

Manufacturing Cost Estimate Table				Annual		Unit	
Fixed capital, C_{FC}		$7,914,044.98					
Working capital (10-20% of fixed capital), C_{WC}		$1,187,106.75					
Total capital investment, C_{TC}		$9,101,151.73					
Manufacturing Expenses							
Direct				$/yr	$/yr	$/m3	$/m3
Raw materials				$0.00		$0.00	
By-product credits	(hydrogen off-gas)			$496,000.00			
Catalysts and solvents				$3,368,358.52		$385.17	
Operating labor				$694,804.25		$79.45	
Supervisory and clerical labor (10-20% of operating labor)				$104,220.64		$11.92	
Utilities							
Steam	kg/y	32 barg @		$0.00		$0.00	
Electricity	kWh @	0.098978 $/kWh		$0.00		$0.00	
Process water	63945 m³ @	1.39946 $/m³		$89,488.44		$10.23	
Water treatment	157500 m³ @	0.088139 $/m³		$13,881.83		$1.59	
Cooling water	315630 m³ @	0.066443 $/m³		$20,971.33		$2.40	
Gas emissions	10406880 m³ @	0.009191 $/m³		$95,647.82		$10.94	
Waste disposal	7586160 kg @	0.2398 $/kg		$1,819,161.17		$208.02	
Maintenance and repairs (2-10% of fixed capital)				$395,702.25		$45.25	
Operating supplies (10-20% of maint & repairs)				$59,355.34		$6.79	
Laboratory charges (10-20% of operating labor)				$104,220.64		$11.92	
Patents and royalties (0-6% of total expense)				$529,651.21		$60.57	
Total, A_{DME}					$7,295,463.43		$834.23
Indirect							
Overhead (payroll and plant), packaging, storage (50-70% of op. Labor+supervision+ maint.)				$716,836.28		$81.97	
Local taxes (1-3% of fixed capital)				$158,280.90		$18.10	
Insurance (1-2% of fixed capital)				$158,280.90		$18.10	
Total, A_{IME}					$1,033,398.08		$118.17
Total manufacturing expense, $A_{ME} = A_{DME} + A_{IME}$					$8,328,861.51		$952.40
General Expenses							
Administrative costs (25% of overhead)				$179,209.07		$20.49	
Distribution and selling (10% of total expense)				$1,059,302.42		$121.13	
Research and development (5% of total expense)				$529,651.21		$60.57	
Total general expense, A_{GE}					$1,768,162.70		$202.19
Depreciation (approximately 10% of fixed capital), A_{BD}					$791,404.50		$90.50
Total Expenses, A_{TE}					$10,097,024.21		$1,154.59
Revenue from Sales	kg/yr @	$/kg), A_s			$10,876,922.45		$1,243.77
Net annual profit, A_{NP}					$779,898.23		$89.18
Income taxes (net annual profit times the tax rate), assume 35%					$272,964.38		$31.21
Net annual profit after taxes ($A_{NP} - A_{IT}$), A_{NNP}					$506,933.85		$57.97
			ertax rate of return, i = (1.5 A_{NNP}/C_{TC}) x 100 =		8.35499506 %		

5.0 Discussion of Results

As shown by the cost estimate tables, this process can be run profitably. This is predicated on three basic assumptions: old batteries can be sourced for free, all equipment can be purchased according to Ulrich's cost information, and hydrogen gas can be used as a credit towards electric costs. In practical use, some of these cost estimates may be slightly altered, but a margin of more than $500 million annually is a promising sign that even with discrepancies in price point, this operation can be run successfully. This process is dually valuable because of its retention of highly valuable materials, including cobalt, lithium, and manganese. These metals are becoming increasingly valuable, meaning this process has the potential to become even more lucrative as the global demand for these elements rises further.

6.0 Conclusions

Based on initial proof of concepts for the separation of LIB from recycled materials proven by Castillo, it was determined that LiOH could be readily extracted from a random mixture of battery compositions in a highly effective manner via hydrometallurgical methods.

7.0 Recommendations & Future Studies

Clearly, the recovery of valuable elements, like Lithium, from recycled materials, like batteries, represents a viable industry within green and renewable energy chemical processes. This study and the economics surrounding our findings was conducted on LMO batteries (Lithium Manganese Oxide) and the common elemental compositions used in our mass and energy balances were based off of a typical composition found within a LMO battery. As shown in Figure 4, the advancement of this specific industry has led to the development of even more advanced batteries

in a variety of additional configurations. One such battery, the NMC (Lithium Nickel Manganese Cobalt Oxide) battery contains a wide mixture of elements but has a much larger specific energy than the batteries studied in this paper. At high temperatures, LMO batteries begin to have lower life spans and lower charging capacities (Heidari). On the other hand, NMC batteries are built in a layered structure to increase its charging capacities. Even more efficient than NMC batteries are NCA LIBs (Lithium Nickel Cobalt Aluminum Oxide). Figure 9 highlights a web of features across these batteries and how they might compare to one another [13].

(a) LMO Batteries   (b) NMC Batteries   (c) NCA Batteries
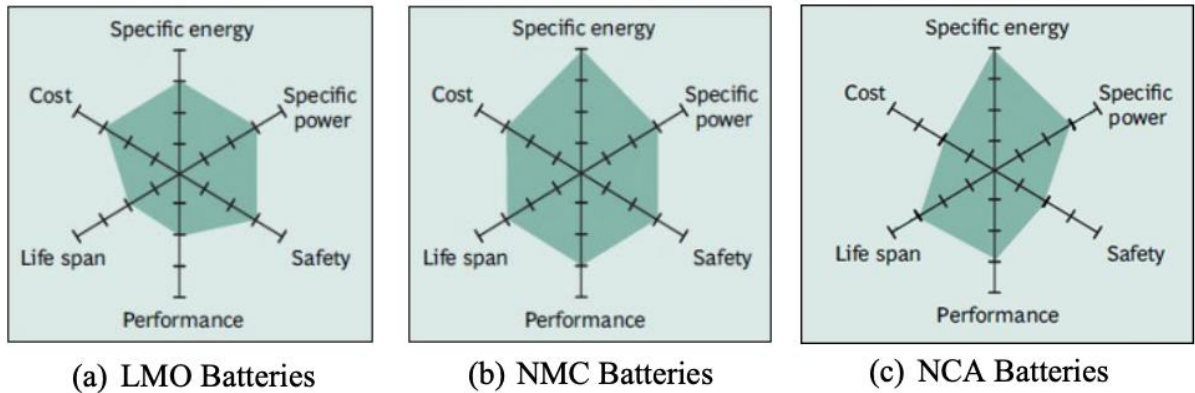
Figure 9: Feature Comparisons Across a Variety of LIBs

In the future, it would be highly beneficial to conduct additional techno-economic study level designs on the more efficient NMC and NCA batteries. It is clear that these batteries are capable of achieving high storage capacities due to their high specific energy and are more affordable. This would align our standards and procedures with current electrochemical findings and make us more competitive as a chemical plant selling to the LIB market.

8.0 References

[1] Castillo, S., F. Ansart, C. Laberty-Robert, J. Portal, "Advances in the Recovering of Spent Lithium Battery Compounds," J. of Power Sources 112. 247-254 (2002)

[2] Lee, C.K., and K.-I. Rhee, "Preparation of LiCoO2 from spent lithium-ion batteries", J. of Power Sources 109. 17-21 (2002)

[3] Liu, C., J. Lin H. Cao, Y. Zhang, Z. Sun, "Recycling of Spent Lithium-Ion Batteries in View of Lithium Recovery: A Critical Review", J. of Cleaner Production 228, 801-813 (2019).

[4] Heidari, K.H., A. Kamyabi-Gol, M.H. Sohi, A. Ataie, Electrode Materials for Lithium Ion Batteries: A review, J. of Ultrafine Grained and Nanostructured Materials, 51(1), 1-12, (2018)

[5] Xu, J., H.R. Thomas, R.W. Francis, K.R. Lum, J. Wang, B. Liang, "Review of Processes and Technologies for the Recycling of Lithium-Ion Batteries", J. of Power Sources 177, 512-527 (2008)

[6] Zeng, Z., J. Li, N. Singh, "Recycling of spent Lithium-Ion Battery: A Critical Review", Critical Reviews in Environmental Science and Technology, 44(10) 1129 - 1165 (2014)

[7] Material Safety Data Sheet, Lithium Ion Batteries (LIBs), *Ideal*

[8] Material Safety Data Sheet, Nitric Acid, *Thermo Fischer Scientific*

[9] Material Safety Data Sheet, Lithium Hydroxide, *LTS Research Laboratories, Inc.*

[10] Material Safety Data Sheet, Sodium Hydroxide (Solid), *Thermo Fischer Scientific*

[11] Sinnott, R K, and Gavin P. Towler. *Chemical Engineering Design: Ray Sinnott, Gavin Towler*. New Delhi: Elsevier, 2010. Print.

[12] Ulrich, Gael D, Palligarnai T. Vasudevan, and Gael D. Ulrich. Chemical Engineering Process Design and Economics: A Practical Guide. Durham, N.H: Process Pub, 2004. Print.

[13] Buchmann, Isidor. "BU-205: Types of Lithium-Ion." *Types of Lithium-Ion Batteries – Battery University*, batteryuniversity.com/learn/article/types_of_lithium_ion.

[14] Choubey, P., Chung, K.-S., Kim, M., Lee, J., & Srivastava, R. R. (2017). Advance review on the exploitation of the prominent energy-storage element Lithium. Part II: From sea water and spent lithium ion batteries (LIBs). *Minerals Engineering*, *110*, 104–121.

[15] Counce, Robert. CBE 488 Lithium Recovery Project Description. *Canvas Instructure*. 2020.

9.0 Appendices

Appendix A: Project Assumptions

The following assumptions were made for the purposes of completing this techno-economical report:

1. Spent LIB batteries could be obtained at a negligible cost ($0/ton)

2. Each reactor and tank vessel was designed under the assumption of an average residence time per/unit operator of 2 hours.

3. In the elemental composition of our batteries, we assumed an even distribution between button cell batteries and cylindrical cell batteries.

4. When sizing the heat exchangers used in our process flow diagram, the heat transfer coefficient of the lithium rich solution was assumed to be 1600 W/K-m²

5. The nitric acid composition used in the separation process was assumed to be 68% based off of available cost information

6. The ChE Index was assumed to be 599.5 as of late 2019.

7. The flow rate of LIBs was assumed to be 1,000 kg/hour and all of the necessary equipment was sized accordingly.

8. Excess heat generated from the crushing of the LIBs prior to the acidification step was deemed negligible in design considerations and cost considerations.

Appendix B: Mass & Energy Balances Table

Species	MW	Process IN (mols/hr)	Process IN (kg/hr)	Process OUT (mols/hr)	Process OUT (kg/hr)	% Loss
Iron	55.85	6741	376.48	6740.94	376.48	0.00%
Cobalt	58.93	16.9	1.00	16.5	0.97	-2.37%
Lithium	6.941	2377.2	16.50	2377.2	16.50	0.00%
Mangannese	54.94	2366.3	130.00	2359.21	129.61	-0.30%
Chromate	52.00	1846.3	96.01	521.266	27.11	-71.77%
Nickle	58.69	715.6	42.00	713.825	41.89	-0.25%
Total			661.99		592.57	-10.49%

	Outlets					Inlets
	Ferric Hydroxide	Ni/Co Hydroxide	Manganese Hydroxide	Sodium Chromate	LiOh to Evap.	Metalic Solids
Stream Parameters						
Temperature (°C)	88.5579	96.0274	100.915	120	105	25
Pressure (atm)	1	1	1	1	1	1
pH					12.61	
Moles, True (mol/hr)	6740.94	730.334	2361.83	519.11		14110.2
Moles, Apparent (mol/hr)	6740.94	730.334	2361.83	519.11		14110.2
Mass (g/hr)	7.20E+05	67975.9	2.10E+05	84082	2.89E+05	6.66E+05
Volume (L/hr)	211.868	16.4007	64.4693	0	238.91	115.367
Density - Solid (g/ml)	3.40023	4.1447	3.25901	0		5.77673
Enthalpy (cal/hr)	-1.34E+09	-9.35E+07	-3.89E+08	-1.71E+08	-1.13E+09	0
Components (mol/hr)						
H2O (Water)	-	-	-	-	12559.5	-
-OH (Hydroxide)	-	-	-	-	1098.1	-
Fe (Iron)	-	-	-	-	-	6741
Fe(OH)3 (Bernalite)	6740.94	-	-	-	-	-
Li (Lithium)	-	-	-	-	1191.96	2377.2
LiOH	-	-	-	-	1185.24	-
Mn (Manganese)	-	-	-	-	-	2366.3
Mn(OH)2 (Pyrochroite)	-	-	2359.66	-	-	-
Cr (Chromium)	-	-	-	-	-	1846.3
Ni (Nickel)	-	-	-	-	-	715.6
Ni(OH)2 (Theophrastite)	-	713.825	1.77461	-	-	-
Na2CrO4	-	-	-	519.11	-	-
Mo (Molybdenum)	-	-	-	-	-	46.9
MoO4	-	-	-	-	46.9	-
Co (Cobalt)	-	-	-	-	-	16.9
Co(OH)3	-	16.5048	0.394032	-	-	-

Appendix C: Equipment Cost Sample Calculations

Equipment Sizing Example Calculations:

A. **Crusher:** In order to size this piece of equipment, all that is necessary to know is the incoming mass flow rate.

$$\dot{m} = 0.277 \ kg/sec \ \text{(from OLI flowsheet)}$$

B. **Reactors:** In order to size this piece of equipment, all that is necessary to know is the volume of the vessel.

$$Volumetric \ flow \ in = 115.367 + 4518.09 + 96.9637 \frac{L}{hr} = 4730.42 \frac{L}{hr} \ \text{(from OLI flowsheet)}$$

Assume a residence time of 2 hr.

$$V = 4730.42 \ \frac{L}{hr} \cdot 2 \ hr = 9460.84 \ L = 9.46 \ m^3$$

The diameter of the reactor was fixed at 1 m and assuming a cylindrical vessel this results in a reactor height of:

$$V = \pi r^2 h \ or \ h = \frac{V}{\pi r^2} = \frac{9.46}{\pi(0.5)^2} = 12.045 \ m$$

C. **Process Vessel:** In order to size this piece of equipment, all that is necessary to know is the volume of the vessel.

$$Volumetric \ flow \ in = 4149.16 \frac{L}{hr} \ \text{(from OLI flowsheet)}$$

Assume a residence time of 2 hr.

$$V = 4149.16 \ \frac{L}{hr} \cdot 2 \ hr = 8298.32 \ L = 8.29 \ m^3$$

The diameter of the reactor was fixed at 1 m and assuming a cylindrical vessel this results in a reactor height of:

$$V = \pi r^2 h \ or \ h = \frac{V}{\pi r^2} = \frac{8.29}{\pi(2)^2} = 10.565 \ m$$

D. Filters: In order to size this piece of equipment, all that is necessary to know is the incoming mass flow rate.

$$\dot{m} = 1.42 \; kg/sec \text{ (from OLI flowsheet)}$$

E. Heat Exchangers: In order to size this piece of equipment, all that is necessary to know is the surface area of the heat exchanger.

$$Q = UA\Delta T_{LM}$$

$$A = \frac{Q}{U\Delta T_{LM}}$$

Obtaining values from OLI flowsheet and assuming a heat transfer coefficient $U = 1600 \; \frac{W}{m^2 K}$, the following area was obtained:

$$A = \frac{13{,}565{,}364.8 \; J/mol}{\left(1600 \; \frac{W}{m^2 K}, \right)(31.91 \; K)} = 265.645 \; m^2$$

Assuming a tube length of 5 meter and a radius of 0.25 m, this would result in the following number of tubes.

$$A = 2\pi r l * n \rightarrow n = \frac{A}{2\pi r l} = \frac{265.645 \; m^2}{2\pi(0.25)(5)} = 33.8 \; tubes$$

F. Tanks: In order to size this piece of equipment, all that is necessary to know is the volume of the vessel. (The tanks were sized in the same way as the reactors and the process vessels, assuming a residence time of 2 hrs)

Appendix D: Chemical Data

    1. *Lithium Ion Batteries*

a.   Physical Hazards: Under normal storage conditions, the solid electrode and liquid electrolyte material are non-reactive provided the integrity of the battery structure and casing.

b.   Chemical Hazards: Wear suitable gloves, avoid contact with skin, and wash with plenty of water if exposed to eyes.

c.   Special Exposure Hazards: Contents of a ruptured LIB can cause respiratory tract irritation and edema. Do not ingest or inhale to avoid throat and gastro/respiratory irritation effects.

d.   Handling & Storage: When storing LIBs, do not let the battery terminals come into contact with one another. Avoid storing in a place prone to static electricity.

e.   Stability & Reactivity: Combustible vapors are prone to form in fire. Avoid crushing and heating without proper conditions in place.

f.   Toxilogical Information: LIBs contain no toxic materials.

    2. *Sodium Hydroxide*

.   Prone to burning, eye and skin damage.

a.   Hygroscopic

b.   Can cause blindness, chemical conjunctivitis, and corneal damage

c.   Stable at room temperature

d.   May decompose into toxic fumes of Sodium Oxide.

    3. *Nitric Acid*

.   Hazard Statements: May intensify fires and is an oxidizer. Can cause eye damage and skin irritation. Corrosive.

a.   In case of fire, use CO_2, dry chemicals, or a foam to extinguish

b.   Avoid ingestion, inhalation, or skin contact

c.   Store in appropriate containers in a cool, well-ventilated space.

   4. *Lithium Hydroxide*

.   Can cause severe eye and skin damage (burns)

a.   Non-flammable

b.   Store in a cool, dry place in a sealed container

c.   Reacts with oxidizing agents, acid, and water

d.   Low Toxicity

Appendix E: Hydrogen Energy Recuperation Calculations

The exhaust from reactor 1 emits roughly 14000 mol/hr of hydrogen at 98% molar composition. COnverting to total chemical potential energy through combustion:

13937 mol H21 hr*2 g1 mol H2*1 kg1000 g*140 Mj1 kg = 3941 Mj/hr

Or 1.095 MW. Generators around this size have an efficiency of about 50 and a gearbox efficiency of 94%, resulting in a working output of 515 kW. At roughly $ .10/kWh for electricity the total energy saved is calculated:

515 kW*8766 hr/yr *.1 $1 kWh=496,000 $/yr

The recommended capitol install costs for generators about this size is roughly 900$/kW output or 463,000 $. This means that this unit will easily pay for itself within a year.

https://www.turbinesinfo.com/steam-turbine-efficiency/

Appendix F: Capital Cost and Manufacturing Cost Sample Calculations

Capital Costs

Heat Exchanger: Given a 265.64 m^2, carbon steel, hairpin multitube heat exchanger at 10 barg, the base cost can be found using Figure 5.36 of Ulrich's text at $25,000.

$$Target\ Year\ Price = Base\ Material\ Cost \times \frac{Current\ ChE\ Index}{Base\ ChE\ Index} = \$25,000 \times \frac{599.5}{400}$$
$$= \$37,468.80$$

Three factors are used to determine the bare module cost (C_{BM}): material factor, pressure factor, and bare module factor. Material factor (F_M) is determined by the type of material used to construct the equipment. Every piece of equipment was assumed to be carbon steel, giving a material factor of 1. This process was carried out at atmospheric pressure, giving a pressure factor (F_P) of 1. The bare module factor can be calculated using Figure 5.38 in Ulrich's text.

$$C_{BM} = Target\ Year\ Price \times F_M \times F_P \times F_{BM} = \$37,468.80 \times 1 \times 1 \times 3.2 = \$119,900$$

Other equipment used rely on different figures in Ulrich's text, but the calculations follow the same format as the above.

Manufacturing Costs

Raw materials are assumed to cost nothing since LIBs are thrown away and can be gathered for no cost. Solvents, in this case nitric acid and sodium hydroxide, are the primary input costs. An operating factor of 0.94 was assumed to factor in unplanned downtimes.

$$HNO_3\ Cost = \frac{\$300}{ton} \times \frac{1229.58\ kg}{hr} \times 8{,}760\ hr \times 0.94 = \$3{,}037{,}456$$

$$NaOH\ Cost = \frac{\$125}{ton} \times 321.48\frac{kg}{hr} \times 8{,}760\ hr \times 0.94 = \$330{,}902$$

$$Solvents\ Cost = \$3{,}037{,}456 + \$330{,}902 = \$3{,}368{,}358$$

Operating labor can be estimated using Ulrich's Table 6.2 and is based on equipment type and number. The overall process required 1 crusher, 2 evaporators, 3 heat exchangers, 2 reactors, 3 LV-separators, and 5 filters.

$$
\begin{aligned}
Operating\ &Labor \\
&= 5 \times (1 \times 0.4 + 2 \times 0.3 + 3 \times 0.05 + 2 \times 0.3 + 3 \times 0.05 + 5 \times 0.05) \\
&\times 41600 \times 1.03^{(2020-2013)} \times 0.94 = \$694{,}804
\end{aligned}
$$

Utilities are the final cost that can be directly calculated. An example utility is process water, which is used in the reaction processes. It was assumed that the process water needed to be at least drinking water quality to avoid corrosion or advanced wear process vessels.

$$
\begin{aligned}
Cost\ per\ m^3 &= 0.002 + 3.0^{-6} \times q^{-0.6} + 0.06 \times Fuel\ Price \\
&= (0.002 + 3.0^{-6} \times 0.00203^{-0.6}) \times 599.5 + 0.06 \times 2.1043 = 1.399\ \$/m^3
\end{aligned}
$$

$$Process\ Water = 63{,}945\ m^3 \times \frac{\$1.399}{m^3} = \$89{,}488.44\ per\ year$$

The remainder of the calculations come from previous estimates. The assumptions needed to make these calculations are noted in parentheses in the Table 4.5.